Assessment of Ring Injectors for Reducing NOx and PM Emissions of Diesel Engines

FINAL REPORT

Hamid R. Rahai, Ph.D.

Center for Energy and Environmental Research and Services (CEERS)
Department of Mechanical and Aerospace Engineering
California State University Long Beach

METRANS contract number 07-221300

August 16, 2010

Disclaimer

The contents of this report reflect the views of the author, who is responsible for the facts and the accuracy of the information presented herein. This document is disseminated under the sponsorship of the Department of Transportation, University Transportation Centers Program, and California Department of Transportation in the interest of information exchange. The U.S. Government and California Department of Transportation assume no liability for the contents or use thereof. The contents do not necessarily reflect the official views or policies of the State of California or the Department of Transportation. This report does not constitute a standard, specification, or regulation.

Abstract

The effects of ring injectors on the performance of a selective catalytic reduction (SCR) system have been investigated. The investigation was divided into two parts. First the mixing effectiveness of circular and rectangular ring injectors on a heated turbulent jet were investigated. The experiments were carried out using a turbulent jet facility at the Center for Energy and Environmental Research and Services (CEERS) laboratory. For this part of the investigation, air was used as both injection and exhaust gases. Results indicate that the ring injector enhances mixing process between the axial flow and the injecting flow with the rectangular injector having a higher mixing effectiveness.

In part two of the investigation, an SCR system with a rectangular two-hole ring injector was developed and the system was tested using the exhaust of a 3-cylinder aspired diesel engine under a moderate shaft loading condition, using ammonia gas as the reducing agent. Results show nearly 80% reductions in NOx emissions. Further study is underway to assess the effect of opposed exhaust flow ammonia injection and tab mixer to identify the best configuration for development of high efficiency automated prototype SCR unit.

Table of Contents

DISCLAIMER	**2**
ABSTRACT	**3**
TABLE OF CONTENTS	**4**
LIST OF FIGURES	**5**
DISCLOSURE	**6**
ACKNOWLEDGEMENT	**7**
BACKGROUND	**8**
MEASUREMENTS PROCEDURE AND TECHNIQUES	**9**
RESULTS AND DISCUSSIONS	**14**
CONCLUSIONS AND FUTURE PLAN	**21**
REFERENCES	**22**

LIST OF FIGURES

Figures **Page**

1. Experimental Set-up……..10
2. Diesel exhaust system ……...…12
3. Ammonia injection system……...12
4. Diesel engine test cell……...…13
5. Axial variation of normalized mean velocity at the jet mid-section for (a)plane jet, (b) jet with ring injector, no injection, (c)Jet with ring, r=0.01, (d) jet with ring, r=0.015, and (e) jet with ring, r=0.02…….15
6. Axial variation of normalized turbulent velocity at the jet mid-section for (a) plane jet, (b) jet with ring injector, no injection, (c) Jet with ring, r=0.01, (d) jet with ring, r=0.015, and (e) jet with ring, r=0.02……...…….15
7. Axial variation of normalized mean temperature (a) plane jet, (b) jet with circular ring, no injection, (c) jet with circular ring, r = 0.01, (d) jet with circular ring, r=0.015, and (e) jet with circular ring, r=0.02…….16
8. Normalized mean temperature contours at x/D=0.08, (a) plane jet, (b) jet with circular ring injector, no injection, and (c) jet with circular ring injector and injection at r=0.02…….16
9. Axial variation of the jet half width and maximum mean velocity for coil-inserted jet with different injection ratios……..……16
10. Contours of normalized streamwise mean velocity at x/D=0.08, (a) plane jet, (b) jet with rectangular ring no injection, (c) jet with rectangular ring and injection, r =0.02…….…….17
11. Contours of normalized streamwise turbulent velocity at x/D=0.08, (a) plane jet, (b) jet with rectangular ring no injection, (c) jet with rectangular ring and injection, r = 0.02……17
12. Axial variation of normalized streamwise mean velocity for (a) plane jet, (b)jet with rectangular ring no injection, and (c) jet with rectangular ring and injection, r =0.02…….……..…17

13. Axial variation of normalized streamwise turbulent velocity for (a) plane jet, (b)jet with rectangular ring no injection, and (c) jet with rectangular ring and injection, r =0.02…….17

14. Axial variation of normalized mean temperature for (a) plane jet, (b)jet with rectangular ring no injection, and (c) jet with rectangular ring and injection, r =0.02…….18

15. Variation of NOx emission with and without ammonia injection ……..19

Disclosure

Project was funded in entirety under this contract to California Department of Transportation.

Acknowledgments

This study was supported with a grant from METRANS applied research program. The author would like to thank METRANS executive committee for their support. The supports of CSULB graduate assistants, Shahab Moayedian and Jae Ji, CEERS technical support staff, and Mr. Mike Fritz and Mr. Joe Wardell, CSULB Mechanical and Aerospace Engineering technicians, are gratefully acknowledged.

1.0. BACKGROUND

Diesel trucks contribute significantly to the statewide emissions from ports and goods movement. According to CARB [1], in 2005, the estimated emissions of NOx and PM from diesel trucks were more than 680 and 30 tons per day respectively. These emissions have resulted in major health impacts which include increased heart disease, respiratory illnesses, cancer risk and premature death. A recent study by Gauderman et al [2] on the effects of pollution on children's health in Los Angles has shown that pollution stunts lung growth in children and can cause premature death or lifelong health problems. In response to these challenges, CARB has proposed strategies with implementation dates between 2006-2020 that can significantly reduce emissions from ports and goods movement activities.

Technologies for reducing emissions from diesel trucks include engine process modifications, exhaust after treatment, use of cleaner fuel, and combinations of these measures. Examples of exhaust after treatments are Diesel Particulate Filters (DPF), Oxidation Reactors, NOx Absorber Catalyst (NAC), Lean NOx Trap (LNT), and Selective Catalytic Reduction (SCR) system. An example of the engine process modification is Exhaust Gas Recirculation (EGR). An overview of these methods and processes are provided by Hefazi and Rahai [3].

DPFs are used to filter out soot or particulate matter. It generally has two chambers, one for oxidation of NO to NO_2 and the second chamber where NO_2 reacts with the particulates to "burn off", converting them to CO, CO_2, and inorganic dusts.

The oxidation reactors are used to convert CO and HC gases into CO_2 and H_2O. It has the potential to remove CO by more than 90% and HC by about 70%. High sulfur reduces the effectiveness of the diesel oxidation catalysts.

The NACs use a base metal oxide with precious metal coating to absorb NOx during the engine lean operation. When the maximum NOx storage condition is met, the catalyst goes through a regenerative process to release the NOx absorbed. The LNT is similar to the NAC without the re-generative process.

In the EGR approach, the exhaust gas acts as a diluents in the air-fuel mixture to lower the combustion rate and temperature, increasing its efficiency and reducing NOx emissions. The maximum EGR fraction is 15-20% of the fuel-air flow rate which limits its capacity to greatly reduce emissions. Thus, multiple methods should be implemented to drastically reduce diesel exhaust emissions.

The introduction of SCR systems using urea as the removing agent has shown to be effective in reducing NOx emissions in diesel engines. Urea is produced by combining ammonia and carbon dioxide at high pressure. It is easy to transport and is a stable solution within normal climatic conditions. When it is injected into the exhaust of a diesel

engine, it is first hydrolyzed to produce ammonia, which reacts with the exhaust gases to produce nitrogen and water.

$$4NO + 4NH_3 + O_2 \rightarrow 4N_2 + 6H_2O$$

$$NO_2 + 4NH_3 + O_2 \rightarrow 3N_2 + 6H_2O$$

Engine out NOx gas emission consists of both NO and NO_2. Therefore, the ratio of the ammonia gas to the exhaust engine out NOx should be determined based on NO-NO_2 ratio of the exhaust gas. To maintain or control this ratio, a diesel oxidation catalyst can be used even though it is not the primary objective.

Reduction of NOx emissions can also be accomplished with a SCR system with hydrocarbons as the reducing agent. The system can use the on-board fuel tank as its reservoir and a control system to time the injection process to the engine timing to optimize the NOx reduction process. Sumiya et al [4] have shown a 30% increase in NOx conversion at a 450 degree C exhaust temperature with diesel fuel sprayed ahead of the catalyst bed.

For a SCR filter, a major factor contributing to the efficiency of the filter is the injecting and mixing processes of the reducing agent. The injection can be in counter flow, co-flow , perpendicular or at an angular direction. Each configuration has a certain mixing property. For example, Yoda and Fiedler [5] and Lam and Chen [6] performed experimental study of counter flowing turbulent jets into a stream with different velocity ratios. Their results indicate that the lateral width of a counter flowing jet, normalized by its penetration distance, decreases with decreasing velocity ratio between the jet and the opposing stream. This indicates a stronger spreading rate which should results in enhanced mixing between the jet and the main flow.

3.0. MEASUREENTS PROCEDURE AND TECHNIQUES

The first part of the study was focused on development of a mixing-injector device for increased mixing between the injected fluid and the exhaust for significant reduction in NO_x emissions. Compressed air was used for both injection and exhaust to find the optimized geometry that can increase the mixing process and to reduce slippage which could enhance the emission reduction process. Part two of the study was focused on laboratory testing of the device for its potential in reducing diesel NOx emissions, using ammonia as the reducing agent.

Part I:

In part I, near-field characteristics of a jet with ring injectors were investigated. The experiments were carried out using a subsonic jet facility at the CEERS laboratories. Figure 1 shows the jet configuration.

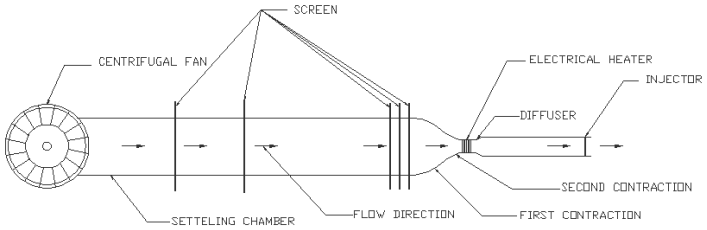

Figure 1. Experimental Set-up.

A centrifugal fan provides the air flow. The settling chamber is 132 cm in length and has various screens with different solidity for flow conditioning. The settling chamber is followed by an 11.75:1 contraction, which is 26.7 cm long. Another contraction with 1.4 area ratio and 15 cm in length is followed to match the cross section of an Omega air heater model AHF-06120. The electric heater is followed by a 1.3 area ratio and 16.5 cm long diffuser. The diffuser is followed by an all Plexiglas tube with 8.255 cm ID and 66 cm in length.

A circular and a rectangular injector were developed. Both injectors were designed to match the inside diameter of the Plexiglas tube. The circular injector was a copper tube ring with its ends connected to compressed air outside through a small wall slot. Its O.D. was approximately 9.5 mm and was pinched at the mid-section to prevent inside air crossing to the other half circle. Each half circle had a hole of approximately 0.8 mm diameter at its mid-section, facing the heated jet in radial direction (similar to a jet in cross flow). Each half-tube was connected independently to a filtered regulated compressed air. Flow rate for each tube was monitored with a Dwyer Instruments direct reading flow meter.

The aluminum rectangular ring had a square cross section with 6.35 mm thickness with two injecting holes of the same diameter as the circular injector facing each other at mid-section. The holes were connected to the regulated compressed air with connecting tubes passing through two holes embedded on the Plexiglas tube behind the ring injector.

The air for the jet flow was heated to approximately 45 C. The maximum mean velocity at the tube outlet was 4 m/sec which corresponds to a Reynolds number based on jet inside diameter of 18,869. Measurements are carried out for plane heated jet, heated jet with ring insert without injection and with injection. For the circular ring injector, the mass flow ratio between the injected air and the heated jet, $r = \frac{\dot{m}_r}{\dot{m}_j}$, were approximately 0.01, 0.015, and 0.02. For the rectangular injector only one mass flow rate ratio of 0.02 was tested.

Measurements of turbulent velocity and mean temperature were made at four streamwise locations of x/D = 0.0.08, 3.0, 5.0, and 8, and various radial locations using a TSI single sensor and an OMEGA Engineering hollow tube J-type thermocouple with 1.5 mm outside diameter. The hot wire was connected to a single channel of IFA 100 intelligent Flow Analyzer and was operated at constant temperature mode at a 1.8

overheat ratio. At each measurement location, 10240 samples were taken and analyzed at a sample rate of 6000 samples per second using an NIUSB-6009 data acquisition unit and Labview software.

The thermocouple was connected to a 14 samples/sec., 24 bit National Instrument temperature module model 9211. A Labview-based program was used to collect the temperature data.

Part II:

An ammonia- SCR system with a ring-injector was developed for injecting ammonia into the exhaust. Figure 2 shows the SCR system. The main components of the SCR system include regulated ammonia gas from a compressed tank, the injector and the catalyst and measurement sensors. Figure 3 shows the ammonia injection system. Two J-type thermocouples were used to monitor exhaust temperature before and after injection. The system allows injection of the ammonia into the exhaust when the exhaust temperature is within an acceptable range for maximum NOx reduction efficiency.

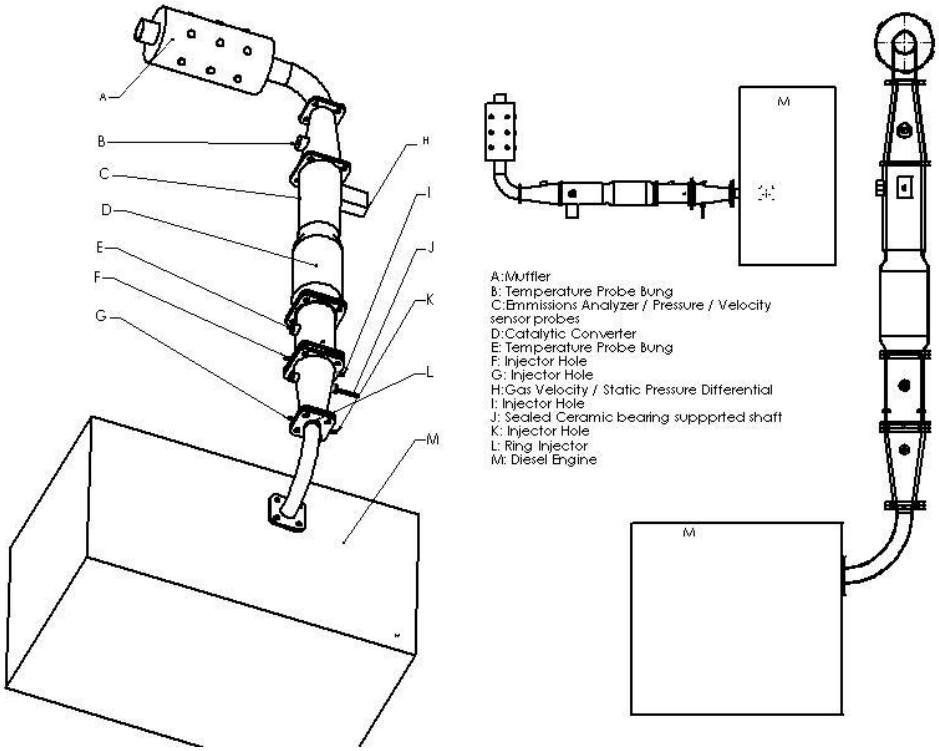

Figure 2. Diesel exhaust system.

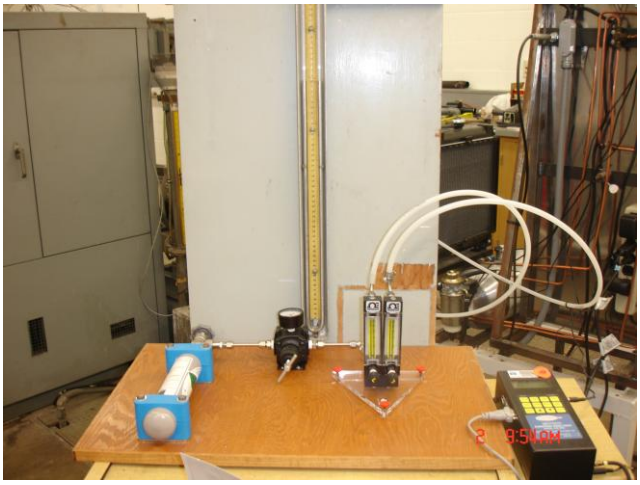

Figure 3. Ammonia injection system.

A Vanguard 3-cylinder liquid-cooled fuel-injected diesel engine with maximum power output of 20 BHP at 3600 rpm was used for the experiments (Figure 4). The engine was run on an electric dynamometer with a moderate load at the output. The engine rpm was at 1650 during all experiments and the exhaust temperature was at 272 ºC during the injection process. Regulated ammonia injection was monitored by two Dwyer Instruments direct reading flow meters.

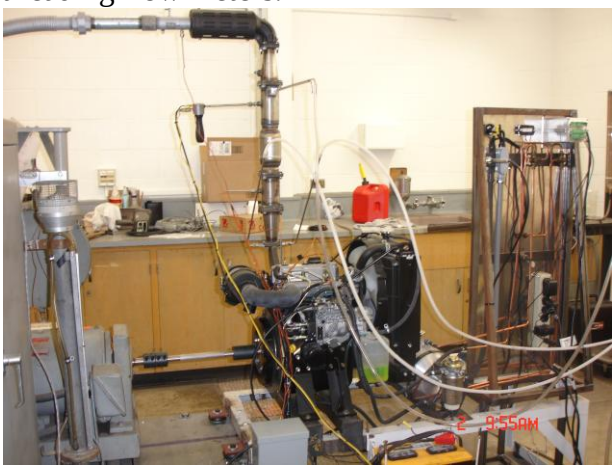

Figure 4. Diesel engine test cell.

The emission data was obtained via a portable ENERAC micro-emissions analyzer model 500 which is capable of measuring accurately the ambient temperature, stack temperature, oxygen, nitric oxide (0-2000 PPM), nitrogen dioxide (0-1000 PPM), carbon monoxide (0-2000 PPM), sulfur dioxide (0-2000 PPM) and stack draft. Other parameters calculated were combustion efficiency, percent carbon dioxide, excess air, oxides of nitrogen, emissions of CO, NO, NO2, NOx, and SO2 in LBS/Million BTU or in

GRAMS/BHH. The unit was connected to a Dell Laptop and data was recorded automatically at 1 minute interval for at least 10 minutes for each operating conditions. Emission measurements were performed downstream of the SCR catalyst at the center of the exhaust pipe. Due to the size of the exhaust pipe, measurements were limited to the center point. The exhaust Reynolds number was in the turbulent flow range and it was assumed due to enhanced mixing process, at the measurement location, the exhaust flow characteristics would be nearly similar to the characteristics of a heated turbulent pipe flow. The exhaust mean velocity was obtained with an S-type tube, connected to a U-tube manometer.

Exhaust NOx measurements were performed without injection and at two ammonia injection rates of 240 and 450 ml per minute.

4.0. RESULTS AND DISCUSSION

Part I:

Figure 5 shows axial variation of the normalized mean velocity for different configurations. Here, the mean velocity is normalized by the maximum velocity at the jet outlet. The mean velocity profiles for the plane jet shows a top hat shape at the jet outlet which changes to a normal profile with merging of the shear layers downstream. When the coil is in place, the top hat profile is diminished and the mean velocity profiles become asymmetric with reduced areas of high velocity, which are indications of higher entrainment and mixing process.

At low injection rate, the regions of high mean velocity is further reduced. With increase in injection, the high velocity region moves away from the centerline toward the edge of the jet and at downstream locations, the profiles become asymmetric with reduced mean velocity gradient. The flow injection from the two jets act similar to the jets in cross flow with superimposed vorticies from flow over the ring. It is most likely that the ring and injections create areas of secondary flow and generation of streamwise vorticity in the near field which enhances the entrainment and mixing process.

Figure 6 shows the corresponding axial variation of turbulence intensity. Here again the turbulent velocity is normalized by the maximum velocity at the jet outlet. For the plane jet, initially there are areas of low intensity which increases with the merging of the shear layers downstream. The presence of the ring generates higher turbulence intensity in the near field. With low injection, the regions of high turbulence intensity move toward the jet boundary and the intensity distribution is asymmetric. With increased injection, the high turbulence intensity regions are displaced to near the edge of the jet at the outlet and decay significantly downstream. These results indicate that the presence of the ring with high injection increases the mixing process in the near field.

Figure 7 shows axial variation of the normalized temperature for different configurations. The mean temperature is normalized by the maximum temperature at the jet outlet. The results show nearly constant normalized temperature distribution at the

outlet which decreases in the downstream locations. The region of high temperature is reduced with placement of the ring inside the jet outlet. The decay and reduction of the temperature gradient become significant with the cold air injection and the temperature distribution become asymmetric at the highest injection rate of r=0.02.

Figure 8 shows contours of normalized mean temperature at x/D = 0.08 for the plane jet, jet with circular ring without inject and jet with circular ring with injection at r=0.02. When ring is in place, the temperature gradient near the jet boundary is reduced and the reduction is more pronounced with injection. Reviewing results for the circular ring injectors indicate that it can enhance mixing between the axial flow and injected flow at high injection ratio, however, mixing is limited to the jet boundary. For this reason, further investigations were focused on a rectangular ring instead. Figures 9-11 show contours of normalized streamwise mean and turbulent velocities and temperature for the plane jet, jet with the square ring with no injection and jet with the square ring and injection at r = 0.02. As the results show the square ring with injection, creates areas of high velocity and turbulence intensity near the center of the jet and higher deformation of the mean temperature with reduced temperature gradient near the jet boundary. These results indicate that the square ring is a better alternative for mixing enhancement which expands to the entire plane of the jet.

Figures 12-14 show axial variation of normalized streamwise mean and turbulent velocity and mean temperature for the jet with and without the square ring and injection. There are significant decay in axial mean and turbulent velocities and temperature which are indications of higher entrainment and mixing process. It seems that the presence of the square ring and injection creates significant increases in axial vortices in the near field which results in high rate of mixing process. Based on these results, a square ring injector with two holes were developed for field testing using the diesel engine test cell.

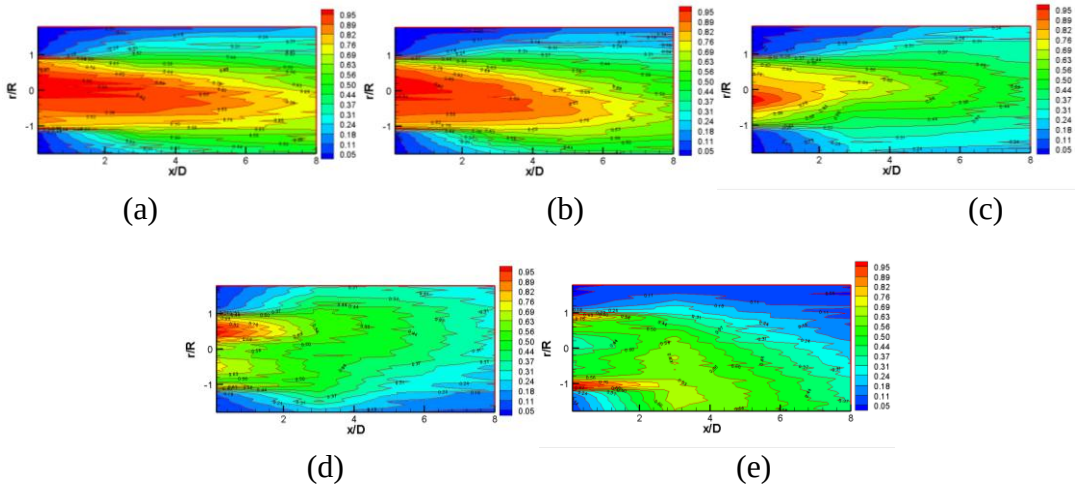

Figure 5. Axial variation of normalized mean velocity at the jet mid-section for (a)plane jet, (b) jet with ring injector, no injection, (c)Jet with ring, r=0.01, (d) jet with ring, r=0.015, and (e) jet with ring, r=0.02.

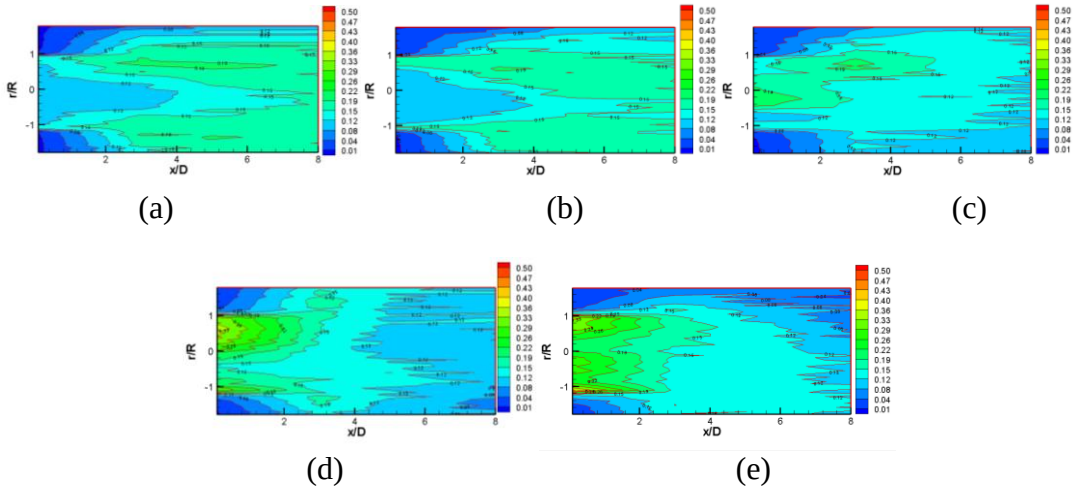

Figure 6. Axial variation of normalized turbulent velocity at the jet mid-section for (a) plane jet, (b) jet with ring injector, no injection, (c) Jet with ring, r=0.01, (d) jet with ring, r=0.015, and (e) jet with ring, r=0.02.

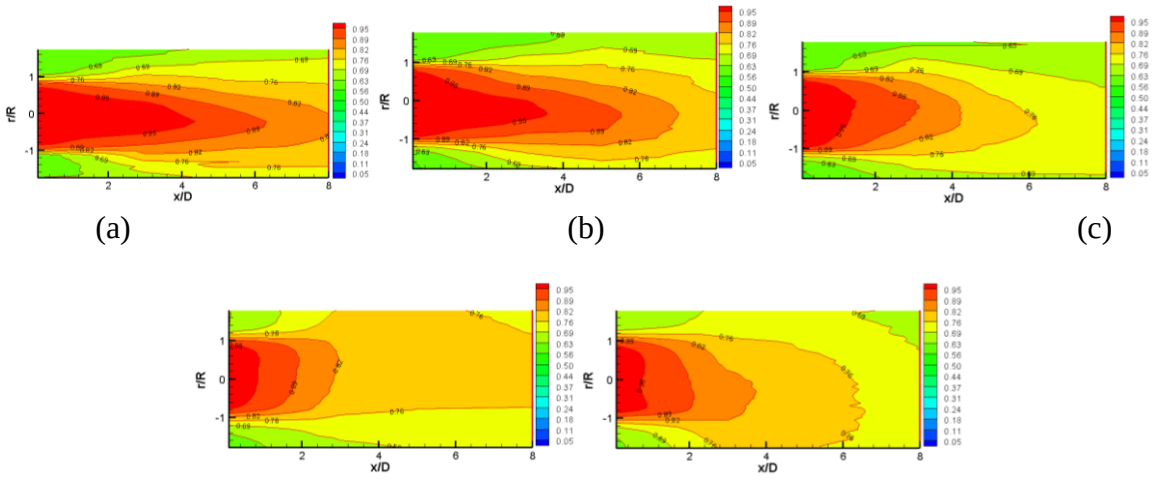

(a) (b) (c)

(d) (e)

Figure 7. Axial variation of normalized mean temperature (a) plane jet, (b) jet with circular ring, no injection, (c) jet with circular ring, r = 0.01, (d) jet with circular ring, r=0.015, and (e) jet with circular ring, r=0.02.

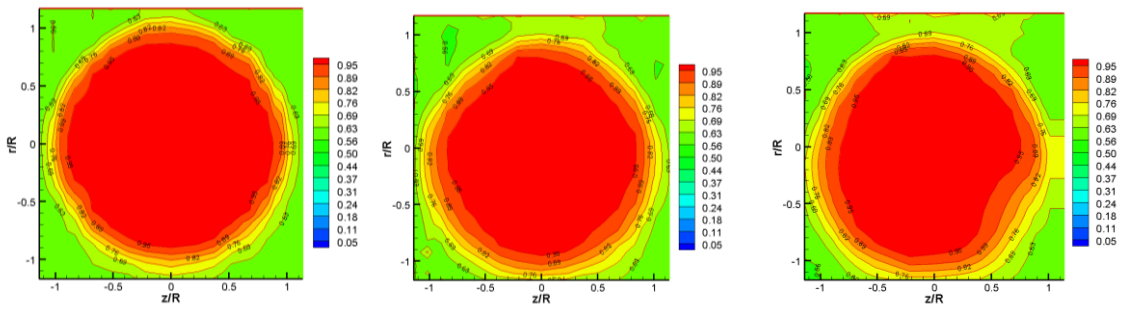

Figure 8. Normalized mean temperature contours at x/D=0.08, (a) plane jet, (b) jet with circular ring injector, no injection, and (c) jet with circular ring injector and injection at r=0.02.

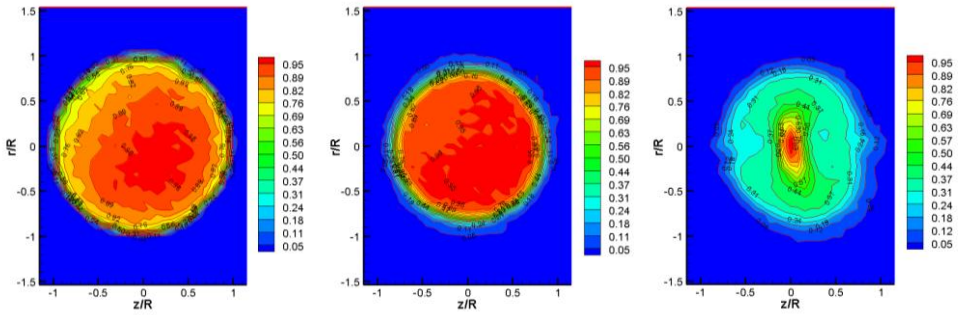

(a) (b) (c)

Figure 9. Contours of normalized streamwise mean velocity at x/D=0.08, (a) plane jet, (b) jet with rectangular ring no injection, (c) jet with rectangular ring and injection, r =0.02.

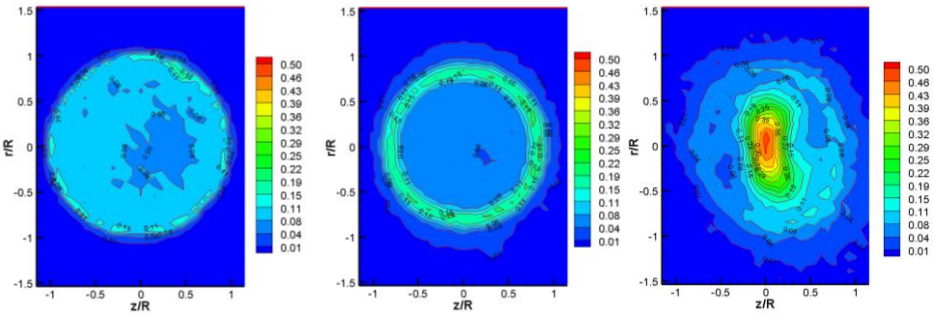

(a) (b) (c)

Figure 10. Contours of normalized streamwise turbulent velocity at x/D=0.08, (a) plane jet, (b) jet with rectangular ring no injection, (c) jet with rectangular ring and injection, r = 0.02.

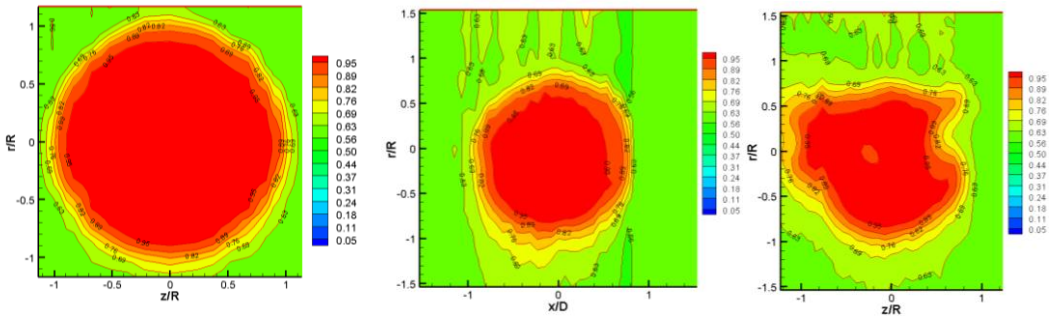

(a) (b) (c)

Figure 11. Normalized mean temperature contours at x/D=0.08, (a) plane jet, (b) jet with rectangular ring injector, no injection, and (c) jet with rectangular ring injector and injection at r=0.02.

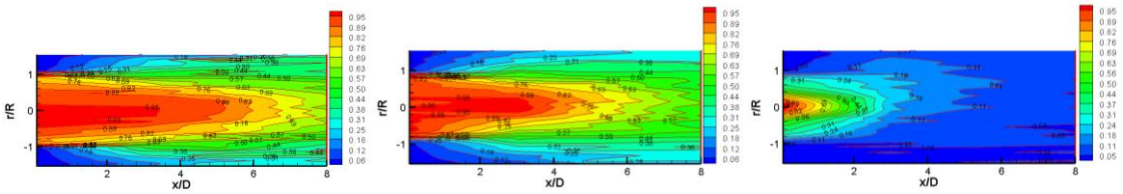

(a) (b) (c)

Figure 12. Axial variation of normalized streamwise mean velocity for (a) plane jet, (b)jet with rectangular ring no injection, and (c) jet with rectangular ring and injection, r =0.02.

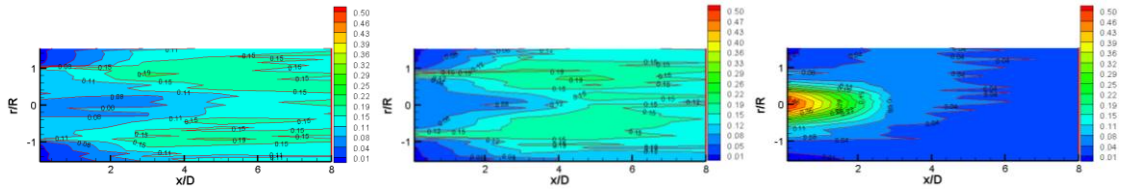

(a) (b) (c)

Figure 13. Axial variation of normalized streamwise turbulent velocity for (a) plane jet, (b)jet with rectangular ring no injection, and (c) jet with rectangular ring and injection, r =0.02.

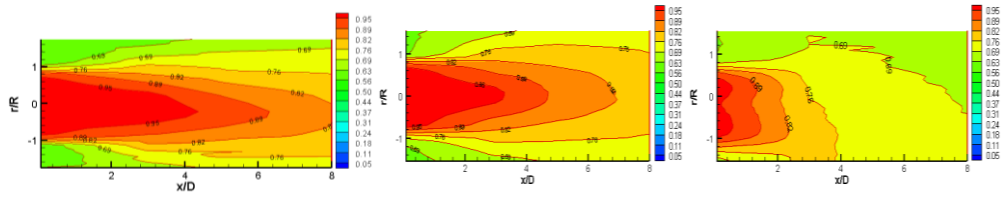

(a) (b) (c)

Figure 14. Axial variation of normalized mean temperature for (a) plane jet, (b)jet with rectangular ring no injection, and (c) jet with rectangular ring and injection, r =0.02.

Part II:

Figure 15 shows diesel NOx without ammonia injection and with ammonia injection at 240 ml/min and 450 ml/min. Initially the engine was tested with a moderate loading condition without ammonia injection for 5-10 minutes duration at 1650 rpm and force at the dynamometer, the amount of fuel consumed, the exhaust pressure differential and emissions were recorded. The resulting break horse power (BHP) and break specific fuel consumption (BSFC) were within 95% of the corresponding values provided by the engine manufacturer. The average NOx without ammonia injection, was approximately at 238 PPM. Considering the exhaust flow rate, based on one to one ratio between ammonia injection and the exhaust NOx, the rate of ammonia injection was estimated to be at about 242 ml/min. However as the results indicate, for a flow rate of approximately 240 ml/min, the amount of NOx reduction is approximately 44%. With increasing in ammonia injection to approximately 450 ml/min., the reduction is nearly 80%. Further increases in ammonia injection resulted in large pressure and temperature drops through the ammonia tubes and phase change. The large pressure and temperature drops were due to the small size of the injecting nozzles which were intended to increase the momentum and penetration of ammonia into the exhaust gas. It should be noted that the ammonia slippage was not measured. It is possible that at high rate of ammonia injection resulted in slippage, preventing maximum reduction in NOx emission.

These results indicate that the square ring injector is a good mixer-injector system and with further optimization of the injecting holes, a simple proto-type injecting system can be developed for significant reduction in NOx emissions of diesel engines, without the ammonia slippage.

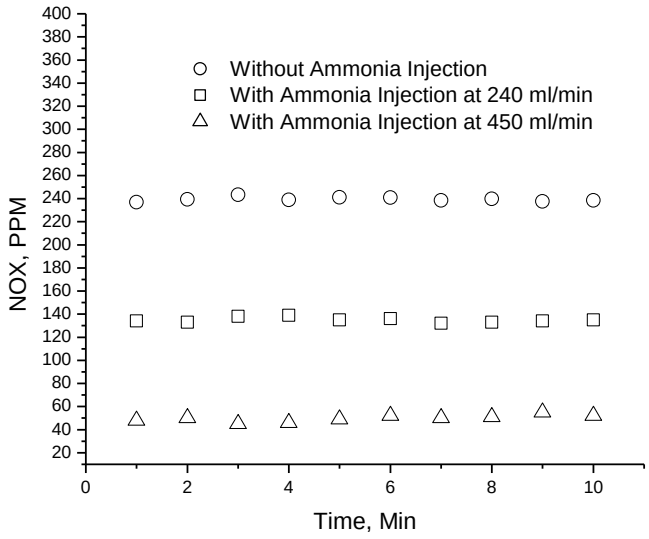

Figure 15. Variation of NOx emission with and without ammonia injection.

5.0. CONCLUSIONS AND RECOMMENDATIONS

The present investigation was divided into two parts. In part one the mixing effectiveness of ring injectors with different injection ratios were investigated using air as both exhaust and injecting fluid. The experiments were carried out in an air-jet facility and mixing effectiveness was investigated using a single hot wire sensor in conjunction with a single channel of TSI IFA-100 intelligent flow analyzer and a small J-type thermocouple. Initially a two-hole circular ring injector with various injection rations, r, of 0.01, 0.015, and 0.02 were investigated. Results indicated a high mixing rate near the jet boundary at the highest injection ratio. To improve the mixing process, a two-hole rectangular ring injector was developed and tested at the 0.02 injection ratio and results indicated significant mixing enhancement within the plane of the jet and downstream. Based on these investigations, a two-hole ring injector was developed for the exhaust of the diesel engine and tested at a moderate engine loading condition with ammonia gas as the NOx reducing agent. Results indicate nearly 44% NOx reduction when the ammonia flow rate is near the NOx flow rate and about 80% reduction with increasing ammonia injection by nearly two fold. Further study is underway to optimize the injecting holes' diameter and development of a prototype unit for maximum reduction in diesel NOx emission. Further study will focus on field testing of the developed system, using a diesel truck.

REFERENCES

1. California Air Resources Board (CARB), "Proposed Emission Reduction Plan for Ports and Goods Movements in California," Released March 21, 2006.

2. Guderman, et al, " The effect of Air Pollution on Lung Development from 10 to 18 Years of Age," The new England Journal of Medicine, Vol. 351, No. 11, September 2004.

3. Hefazi, H., and Rahai, H.R., "Emission Control technologies for Ocean Going Vessels (OGVs)," Final Report, California Air Resources Board (CARB), June 2008.

4. Sumiya, S., Muramatsu, G., Matsumura, N., and Yoshida, K., 1992, "Catalytic Reduction of NOx and Diesel Exhaust," SAE paper No. 920853.

5. Yoda, M. and Fiedler, H.E., 1996, "The Round Jet in a Uniform Counterflow Flow Visualization and Mean Concentration Measurements," Experiments in Fluids, 21, 427-436.

6. Lam, C.H.C. and Chen, K.M., 1998, "Centerline Velocity Decay of a Circular Jet in a Counterflowing Stream," Physics of Fluids, Vol. 10, No. 3, 637-644.